Changes in Electrochemical and Optical Properties of Oligoalkylthiophene Film Induced by Bipolaron Formation

Yutaka Harima,* Rahul Patil, Hongfang Liu, Yousuke Ooyama, Kazuo Takimiya, and Tetsuo Otsubo

Department of Applied Chemistry, Graduate School of Engineering, Hiroshima University, Higashi-Hiroshima 739-8527, Japan

Received: August 28, 2005; In Final Form: November 29, 2005

An unusual electrochemical response is found for oligoalkylthiophene (13T) films in acetonitrile. A pristine 13T film exhibits a stable redox wave in cyclic voltammogram when the anodic potential limit is below 0.6 V, whereas the redox peaks shift clearly to the negative side by ca. 0.1 V once the 13T film experiences a potential beyond 0.7 V. After this electrochemical stimulus is imposed on a pristine 13T film, the absorption and emission spectra change their features. These findings, along with the measurements with varying thicknesses of 13T films, suggest that a pristine 13T film is a mixture of two phases to be oxidized at separate potentials and that one phase can be switched to the other by the potential stimulation. A plausible model proposed for explaining these observations assumes that a key parameter characteristic of the two phases is a conformation of 13T molecules in the solid state and a change in conformation, leading to the shift of the redox potentials and the change of optical properties, is induced by electrochemical generation of bipolarons on the half units of the oligomers in the pristine 13T film.

Introduction

In recent years, extensive studies have developed on π-conjugated oligothiophenes. The main interest stems from their possible applications to molecular electronics, optoelectronics, light emitting diodes, field effect transistors, and photoelectric conversion.[1−8] Synthetic studies have recently been made, intensively aiming at preparation of long oligothiophenes that would act as molecular wires.[9−17] The longest oligothiophene achieved so far consists of 96 thiophene units, and its wire length reaches 37.2 nm.[18] Besides these, oligothiophenes and other π-conjugated oligomers, possessing well-defined molecular lengths and structures, are studied as model compounds for better understandings of electric and optical properties of the corresponding conducting polymers. On the other hand, a series of polymers having alternating units of oligothienylene and oligosilanylene have drawn significant research attention because of a unique interaction between a silicon σ-orbital and a π-electron system called $\sigma-\pi$ conjugation.[19−21] They are also an important class of polymers for studying charge transport mechanisms of conducting polymers because these Si polymers consist of well-defined π-conjugation units bridged by insulating silanylene units, and thus, a possible role of an intrachain transport of charge carriers in the conduction process can be discussed.[22−24] Oligothiophenes themselves could be used for this objective. It is likely, however, that conformation of oligomer chains alters upon oxidation, thus leading to a change in the film structure. In fact, Lapkowski et al. have found reversible changes in morphology of a regioregular sexi-3-alkylthiophene film with the applied potential.[25−28] In our early conduction study, one of the reasons for the use of Si copolymers is to prevent a possible change of the film structure during a redox process by fusing a definite length of oligothiophenes into a single polymer chain.

In the present study, electrochemical and optical properties of thin films of oligoalkylthiophene consisting of 13 thienylene units are investigated to clarify the solid-state natures of the π-conjugated oligomer. A strange redox behavior is found and is discussed in conjunction with a change in the chain conformation induced by the application of potential. Intensive physicochemical studies have already been performed on oligothiophenes and oligoalkylthiophenes in solution. Up to the present time, however, only a few reports are available in the literature on electrochemical properties in their solid states,[25−30] although studies on solid-state properties of π-conjugated oligomers are a prerequisite for their applications to a variety of electronic and optoelectronic devices.

Experimental Section

Oligoalkylthiophene (13T) was synthesized according to the method described earlier.[15] The structure depicted in Figure 1 was confirmed by ^{1}H NMR (400 MHz, $CDCl_3$): $\delta = 0.88$ (m, 24H), 1.32 (m, 80H), 1.66 (m, 16H), 2.77 (m, 16H), 6.93 (d, $J = 5.2$ Hz, 2H), 6.95 (s, 2H), 6.98 (s, 2H), 7.01 (s, 2H), 7.05 (d, $J = 3.8$ Hz, 4H), 7.07 (s, 2H), 7.15 (d, $J = 3.8$ Hz, 4H), 7.17 (d, $J = 5.2$ Hz, 2H). Tetraethylammonium perchlorate (Et_4NClO_4) and acetonitrile (MeCN) were both from Tokyo Kasei. Et_4NClO_4 was purified by recrystallization from ethanol. MeCN was refluxed over P_2O_5 for a couple of hours under N_2 atmosphere and then distilled before use. Au-coated glasses were prepared by use of an electron beam apparatus. A thin layer of Cr (2 nm) was first deposited on a glass substrate prior to evaporation of Au (30 nm). ITO glasses were obtained from Matsuzaki Shinku Co. Metals used were of high purity (>99.99%). Other chemicals were of reagent grade and used without further purification.

Thin films of 13T were prepared by a spin-coating technique at 3000 rpm on Au-coated glasses or ITO electrodes by using

* Corresponding author. E-mail: harima@mls.ias.hiroshima-u.ac.jp.

10.1021/jp054863w CCC: $33.50
Published on Web 01/06/2006

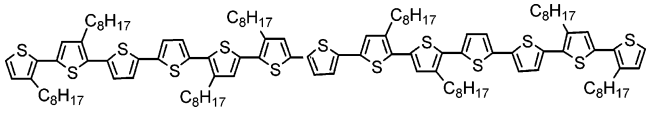

Figure 1. Molecular structure of oligoalkylthiophene (13T).

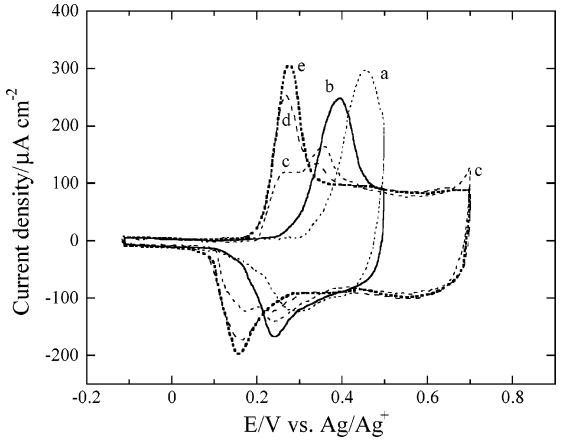

Figure 2. Cyclic voltammograms of a 13T film (40 nm in thickness) on Au electrode in MeCN/Et_4NClO_4 (0.1 M) solution. The potential is cycled at 50 mV s^{-1} between −0.10 to 0.50 V during the first twelve cycles, and the positive potential limit is extended to 0.7 V in further potential cyclings. Curves (a−e) correspond to (a) first cycle, (b) 2nd−12th cycles, (c) 14th cycle, (d) 15th cycle, and (e) 16th and subsequent cycles.

different concentrations of 13T in chloroform. All electrochemical measurements were performed with a three-electrode system consisting of Ag/Ag^+ and Pt wire as reference and counter electrodes, respectively. Cyclic voltammograms (CVs) were recorded in MeCN/Et_4NClO_4(0.1 M) solution by using a Hokuto Denko HAB-151 potentiostat equipped with a function generator. In situ absorption spectra were recorded on a Shimadzu UV-3101PC spectrophotometer. Fluorescence spectra were taken on a Hitachi F-4500 fluorescence spectrophotometer. Atomic force microscopy (AFM) measurements were made with a Shimadzu SPM-9500 scanning probe microscope operated in contact mode with a silicon nitride tip with 200 μm cantilever length and 0.02 N m^{-1} spring constant. All the measurements were made at room temperature.

Results

Figure 2 depicts CV curves of a pristine 13T film measured with two anodic switching potentials. Up to the 12th potential cycle, the switching potential was set at 0.5 V, and for the following cycles, it was extended to 0.7 V. The first potential cycling (curve a) gives redox peaks at E_{pa}/E_{pc} = 0.46/0.30 V, and during the 2nd to 12th cycles (curve b), stable redox peaks are observed at 0.40/0.25 V. The initial shift of the redox potentials seems to be caused by swelling of the 13T film induced by electrochemical doping of anions into the pristine film. The magnitude of the potential shift was reduced for thinner films, supporting this explanation. When the potential is swept for the first time up to 0.7 V (13th cycle, not shown here), a slight increase of anodic currents is found at around 0.65 V, as seen in the next 14th CV curve (curve c). This small current increase disappears for subsequent potential cyclings, and concomitantly, the shape of the redox wave changes with the cycle number gradually (curves c and d). After the 16th and the following cycles (curve e), a stable redox wave appears at 0.28/0.15 V. The change of CV curves was faster when the anodic switching potential was made more positive than 0.7 V.

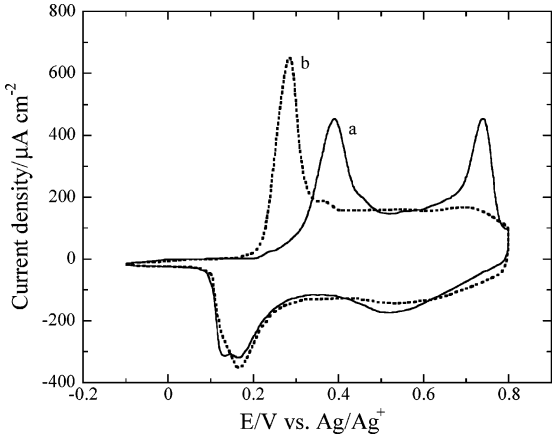

Figure 3. Cyclic voltammograms of a 13T film (60 nm) on Au electrode in MeCN/Et_4NClO_4 (0.1M) solution. The potential is cycled at 50 mV s^{-1} between −0.10 to 0.80 V. Curve (a) is obtained at the first cycle after scanning the potential up to 0.50 V once and curve (b) is for the second and the subsequent cycles.

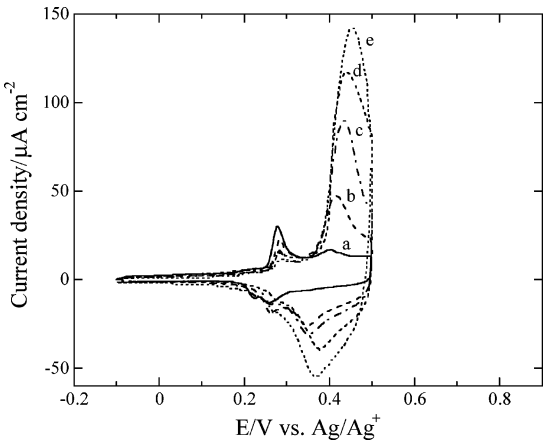

Figure 4. Cyclic voltammograms of varying thicknesses of 13T films on Au electrode in MeCN/Et_4NClO_4 (0.1 M) solution. Thicknesses of 13T films are (a) 3, (b) 6, (c) 10, (d) 15, and 20 nm. The potential is cycled in the range of −0.10 to +0.50 V at 50 mV s^{-1}.

This trend can be noted more distinctly in Figure 3. A pristine 13T film after being cycled once between −0.1 and 0.5 V for swelling of the film shows clearly two oxidation peaks of similar heights at 0.40 and 0.73 V (curve a), being accompanied with one broad and small reduction peak at 0.52 V and almost combined two reduction peaks at 0.1−0.2 V. The small current increase at 0.70 V in curve c of Figure 2 corresponds to a foot of the second oxidation peak in curve a of Figure 3. In the next potential cycling shown by curve b of Figure 3, the second oxidation peak disappears completely, and the first peak gains its height and shifts to the cathodic direction. Curve b has a feature common to CV curves of polypyrrole and polythiophenes films:[31] one oxidation wave is followed by an almost constant oxidation current tail. The shape of the CV curve did not change during subsequent potential cyclings within this potential range.

An influence of thickness of 13T film on the shape of CV curves is summarized in Figure 4, where the potential is cycled between −0.1 and 0.5 V. For the thinnest 13T film (3 nm, curve a), two oxidation peaks are seen at 0.28 and 0.40 V. As the film thickness is increased, the first oxidation peak decays with the growth of the second peak. The thickest 13T film (20 nm, curve e) has a main oxidation peak at 0.45 V, with a small peak at 0.28 V. All these CV curves were stable in this potential range. After the switching potential was raised to 0.80 V, however, the CV curves changed their shapes greatly, as shown

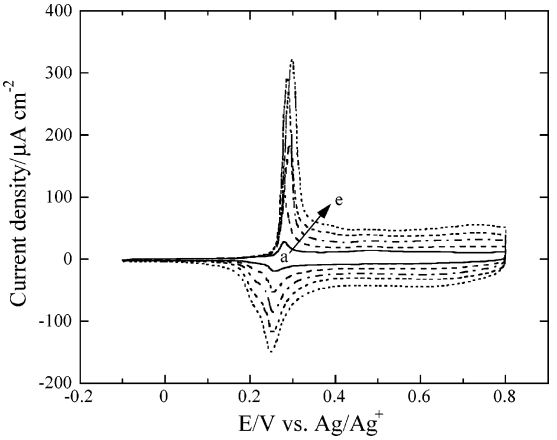

Figure 5. Cyclic voltammograms of varying thicknesses of 13T films on Au electrode in MeCN/Et_4NClO_4 (0.1 M) solution. Thicknesses of the 13T films are the same as in Figure 4. Voltammograms are recorded in the second cycle. The potential is cycled in the range of −0.10 to +0.80 V at 50 mV s^{-1}.

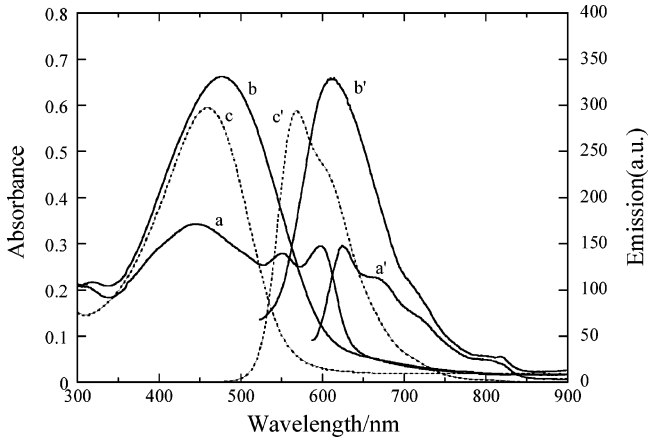

Figure 6. (a), (b) Absorption and (a′), (b′) emission spectra of a neutral 13T film (60 nm) on ITO substrate (a), (a′) before and (b), (b′) after application of potential beyond 0.80 V. (c) Absorption and (c′) emission spectra of 13T in chloroform is represented for a comparison purpuse. Excitation wavelength is 450 nm for all the fluorescence measurements.

in Figure 5. The second peak in each CV curve of Figure 4 disappears and the first peak gains its height in turn. Such drastic changes of CV curves were observed also for 13T films deposited on ITO in place of Au substrate.

Optical properties of a thick 13T film on ITO before and after the electrochemical stimulus are compared in Figure 6, together with absorption and fluorescence spectra of 13T in chloroform (curves c and c′). A pristine 13T film exhibits a broad absorption band at 450 nm (2.78 eV), with two side peaks of 550 and 600 nm (curve a). The energy difference between the two peaks is 0.19 eV, in good agreement with those for equally spaced three side peaks observed with polycrystalline thin films of quaterthiophene, sexithiophene, and octithiophene.[32] Correspondingly, a fluorescence spectrum of the pristine film (curve a′) shows a main peak at 620 nm and a few satellite peaks on the long wavelength side. The same 13T film was oxidized at 0.8 V and then reduced to a neutral state, followed by a thorough rinsing with MeCN. When the 13T film is subject to the potential stimulus, the absorption spectrum changes its feature entirely (curve b), just like the change in shape of CV curves: two side peaks disappear and a single broad absorption band at 475 nm (2.63 eV) similar in shape to curve c for 13T in chloroform gains its height. Likewise, the fluorescence spectrum shows a broad band at 610 nm with a slight structure

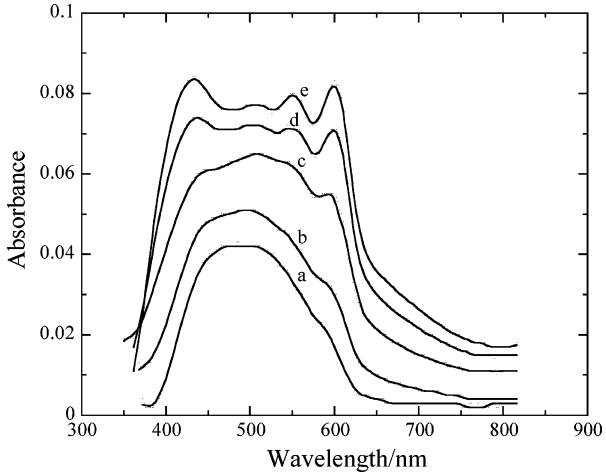

Figure 7. Absorption spectra of varying thicknesses of 13T films on ITO substrate. Thicknesses of the 13T films are the same as in Figure 4.

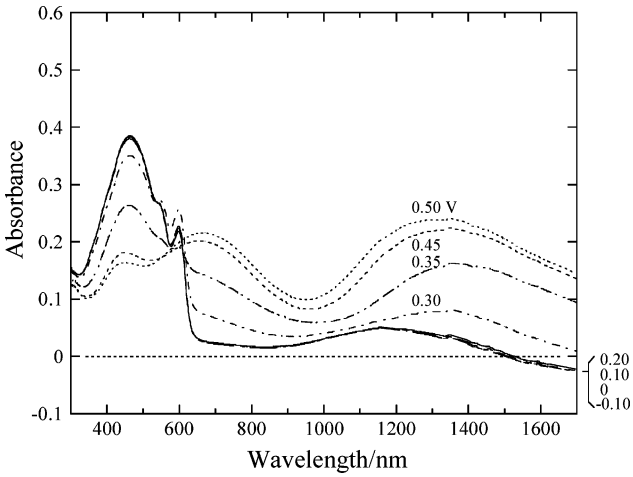

Figure 8. In situ absorption spectra of a pristine 13T film (50 nm) on Au electrode in MeCN/Et_4NClO_4 (0.1 M) solution. Numeral on each curve denotes the potential applied to the 13T film.

on the low energy side (curve b′). Absorption spectra of pristine 13T films with varying thicknesses are depicted in Figure 7. The samples used for the absorption measurements were prepared by using the same solutions as those for CV measurements of Figures 4 and 5. The main absorption band for the thinnest film is located at ca. 500 nm. As the film thickness increases, the main band splits into three peaks at 430, 550, and 600 nm, together with a faint peak at 500 nm. These three peaks in curve e of Figure 7 correspond to those observed in curve a of Figure 6 for the thicker and pristine 13T film. One of the additional findings related to the optical properties of the 13T film is that the side peaks characteristic of thick pristine films disappear by heating the 13T film at ca. 60 °C for more than 10 min, and a single broad band similar to curve b of Figure 6 emerges. In addition, the absorption spectrum of the electrochemically treated film recovered to the one for a pristine film, just by standing the treated film in ambient atmosphere for 2 days or by illuminating it with an intense UV light for several minutes.

In situ absorption spectra of a thick 13T film before and after being biased at 0.8 V are represented in Figures 8 and 9, respectively. The 13T film at potentials of −0.10 to 0.20 V less positive than 0.4 V for the first oxidation peak exhibits absorption spectra consisting of a main band and two side peaks, similar in position to curve a in Figure 6, suggestive of no

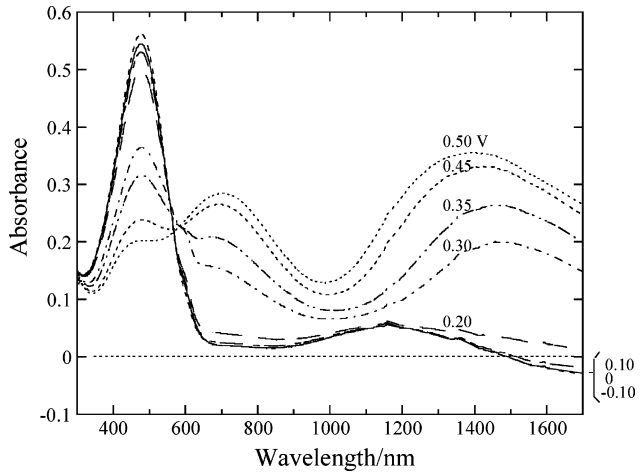

Figure 9. In situ absorption spectra of a 13T film (50 nm) on Au electrode in MeCN/Et_4NClO_4 (0.1 M) solution, obtained after the film is cycled between −0.10 and 0.80 V once. Numeral on each curve denotes the potential applied to the 13T film.

occurrence of any electrochemical oxidation in this potential range. A broad band centered at 1200 nm may be an artifact arising from reflection and/or interference due to the film or glass substrate. The spectral shape starts to change at 0.30 V: the main absorption band decreases simultaneously with the increase of absorbances in the long wavelength region. When the film is biased at 0.35 V, the main band decreases further with disappearance of the side peaks. Absorbances at around 700 nm (1.87 eV) increase, and a broad band at 1360 nm (0.92 eV) becomes evident. The two absorption bands grow as the potential is raised further, although the NIR band slightly shifts to the short wavelength side. A similar spectral change with potential have been observed with a thin film of monosilanylene−oligothienylene copolymer.[23,24] These bands at ca. 650 nm and in the NIR for the copolymer films have been ascribed reasonably to cation radical π-dimers formed between two adjacent oligomer chains. In contrast, the 13T film after being electrochemically treated at 0.8 V has a single absorption band at 480 nm when the applied potential ranges from −0.10 to 0.10 V. As the potential is increased beyond 0.20 V, the absorption spectrum changes its feature drastically. The main band decreases and two additional bands evolve at 700 and 1480 nm (1.79 and 0.84 eV). The 1480-nm band gradually shifts to 1400 nm (0.89 eV) as the potential is increased. The feature of evolution of these additional bands is similar to Figure 8 for the 13T film before the high potential application except for the difference of their onset potentials. It is to be noted that these additional bands are shifted by 0.08 eV to the low energy side after the 13T film was treated at 0.8 V. It is to be commented also that the changes of spectral shapes shown in Figures 8 and 9 are reversible with respect to the change of applied potential.

AFM images of Figure 10 show three different states of a 13T film: (a) before a contact of the 13T film with MeCN, (b) after a potential cycling between −0.10 and 0.50 V, and (c) after a potential sweeping up to 0.80 V. Obviously, the surface of a 13T film after being treated is more rough than the others.

Discussion

Redox potentials for thin films of monosilanylene−oligothienylene copolymers (PS*n*Ts) are plotted in Figure 11 as a function of the number of thiophene units (*n*) in the polymer chain.[24] Here, the redox potential is defined as a midpotential between oxidation and reduction peaks. As *n* increases, redox potentials for the second oxidation step decrease regularly, while those for the first step are almost constant except for PS5T. It is well evidenced by spectroelectrochemistry that the first and second oxidation steps correspond to the formation of polarons and/or π-dimers, and bipolarons, respectively.[24] For relatively thick and pristine 13T films before electrochemical stimulus, on the other hand, the redox potential for the first step is located at 0.32 V (see curve b of Figure 2). This potential value is in good agreement with those of the first step for PS*n*Ts with $n \geq 6$, indicating that the formation of polarons and/or π-dimers is responsible for the first oxidation step for pristine 13T films. Along with the first oxidation peak, curve a of Figure 3 clearly demonstrates the second peak with a height similar to the first one. The redox potential for the second step is 0.62 V close to the one for PS7T, or between PS6T and PS8T. It is inferred from the close agreement of redox potentials that the second oxidation step in the 13T film is ascribable to the generation of bipolarons on oligothienylene units whose effective π-conjugation length is much shorter than a full unit of 13T, or rather close to a half of 13T. Once bipolarons are generated, the 13T film never exhibits the second redox wave afterward, and the first redox wave shifts to a less positive side. The negative shift of the redox potential suggests that the 13T film after bipolaron generation consists of more extensively conjugated oligothienylene units than the pristine 13T film. As an extension of our previous mobility study with PS*n*Ts,[24] a series of PS*n*Ts with longer oligothienylene units were recently synthesized.[33] Redox potentials for the first step were 0.46, 0.32, 0.31, 0.27, and 0.26 V for newly synthesized PS7T, PS8T, PS10T, PS12T, and PS14T, respectively, showing a negative shift of the redox potential with the increase in the length of oligothienylene unit. A similar shift of redox potentials has been reported for a series of end-capped oligothiophenes in solution.[34−36] An alternative explanation for the shift of redox potentials is dimerization of 13T, as observed by Heinze et al., with a *p*-sexiphenyl oligomer in CH_2Cl_2/Bu_4NPF_6 (0.1 M).[29] To examine this possibility, a derivative of 13T with methyl groups at both ends was synthesized. Methyl groups at the end positions are well-known to prevent the dimerization process.[37] CV measurements revealed that voltammetric features of both 13T and end-capped 13T films were exactly the same with each other, indicating that the dimerization process in the free-end 13T film does not occur and can be ruled out as the reason for the redox potential shift. As shown by curve a of Figure 3, cathodic currents due to reduction of bipolarons in the reverse scan are obviously small compared with those observed for PS6T.[24] As Figure 11 shows, the first and second redox potentials tend to merge when the number of thiophene units in PS*n*T is larger than 10. In view of this and the extension of π-conjugation length caused by bipolaron formation, bipolarons generated in the second oxidation step may change immediately into another species that can be reduced at less positive potentials.

When 13T films are much thinner than 40 nm, two oxidation peaks are simultaneously noted in the potential range up to 0.5 V (Figure 4). It is worthy to note here that positions of the two redox potentials correspond well to those for the first oxidation step of a 13T film before and after bipolaron formation. Relative height of the 0.4−0.5 V peak to the 0.28 V one increases with the increase in the film thickness, and the former peak becomes predominant for the 20-nm-thick 13T film. After sweeping the potential up to 0.8 V once, the 0.4−0.5 V peak disappears completely and the 0.3 V peak is enhanced in turn, as shown in Figure 5. These findings demonstrate that a pristine and

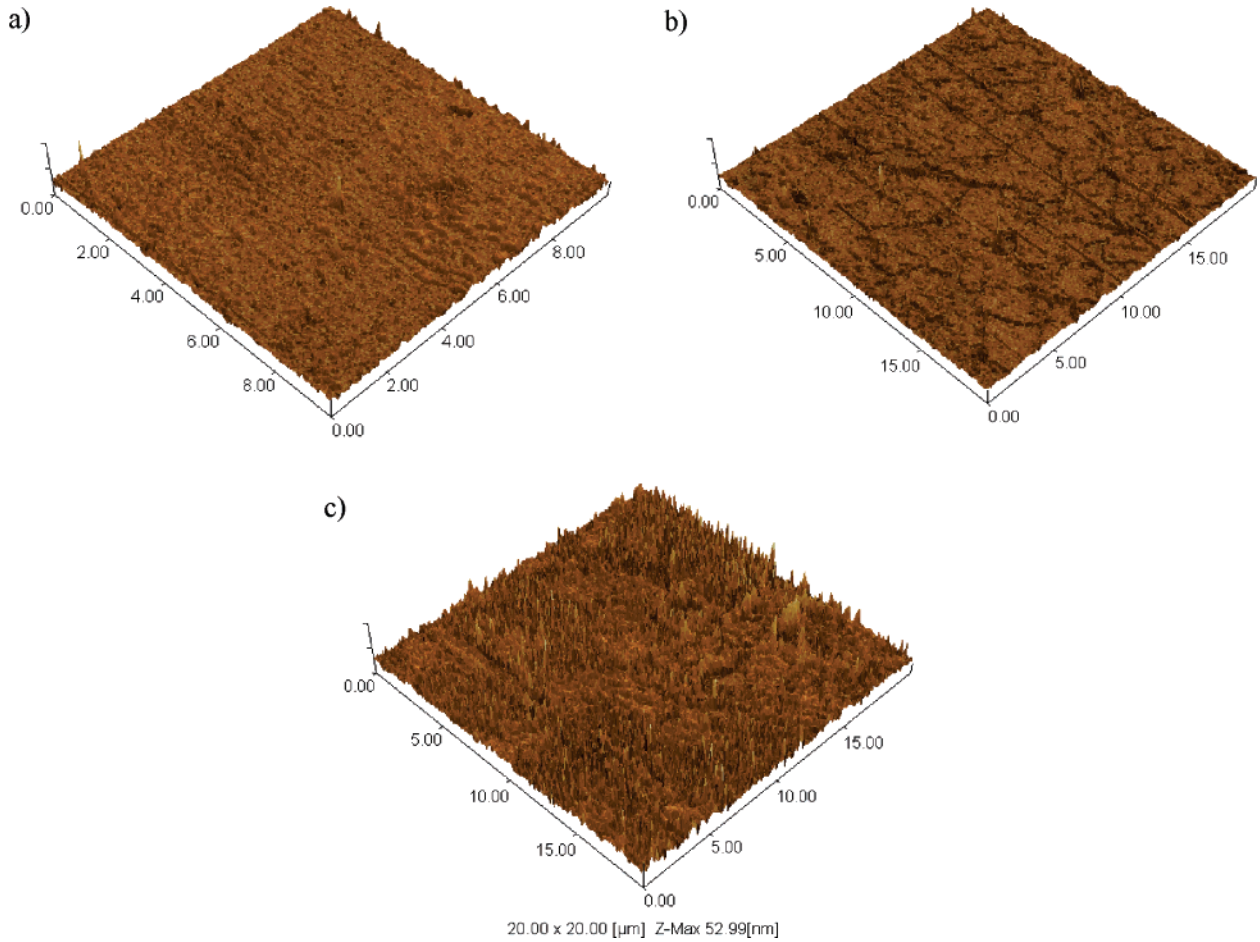

Figure 10. AFM images of a neutral 13T film (a) before contact with MeCN, (b) after cycling the potential between −0.10 and 0.50 V, and (c) after scanning the potential up to 0.80 V. The 13T film after the electrochemical treatment was rinsed with MeCN and dried in air.

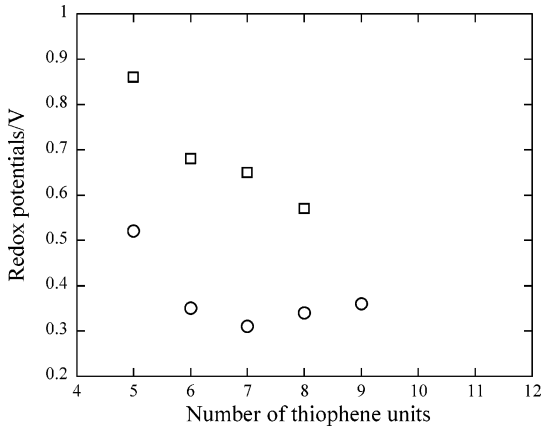

Figure 11. Redox potentials of monosilanylene−oligothienylene copolymers (PS*n*Ts) against the number of thiophene units in the chain for (a) the first and (b) the second oxidation steps.

relatively thick 13T film is a mixture of two phases, I and II, consisting of oligothienylene units with different effective π-conjugation lengths corresponding to half and full units of 13T, respectively. Furthermore, the fraction of the two phases depends on the film thickness, and thicker 13T films consist mainly of phase I containing a half unit of the full π-conjugation length of 13T. This view is consistent with a change of a spectral pattern for 13T films with the film thickness, as will be discussed later in more detail. Combining the above observations leads us to a conclusion that, by being oxidized to generate bipolarons, phase I of shorter conjugation units (a half of 13T) is transformed to phase II, comprising longer conjugation units (a full length of 13T).

Enhancement of a π-conjugation length due to the bipolaron formation in the 13T film will be evidenced further by in situ spectroscopic measurements with a thick 13T film shown in Figures 8 and 9. With a 13T film without the experience of the bipolaron formation, two absorption bands evolve at 0.92 and 1.87 eV upon oxidation of the film at 0.35 V, and oxidation at more positive potentials results in a slight shift of the 0.92 eV band to 0.96 eV. The positions of the absorption bands and the trend of the band shift with oxidation potential are similar to those for cation radical π-dimers in PS6T film.[24] For the 13T film after bipolaron formation, on the other hand, oxidation of the same 13T film at a potential of 0.30 or 0.35 V gives two absorption bands at 0.84 and 1.79 eV, both energies being lower than those for the pristine film. It is known that longer π-conjugation units give absorption bands on the low energy side. This trend is also true for π-dimers in thin films of a series of PS*n*Ts.[24] In view of these, one can presume that the effective π-conjugation length in the treated 13T film is longer than the half unit of 13T involved in the pristine film and this change is caused by electrochemical generation of bipolarons. It is seen from Figures 8 and 9, or more clearly from Figure 6, that the main absorption band of the neutral 13T film shifts from 450 to 475 nm after bipolaron formation. This provides a further support for enhancement of the effective π-conjugation length by electrochemical generation of bipolarons.

A final remark to be discussed is a change of optical properties of 13T films before and after bipolaron formation. Absorption spectra of neutral films of poly(3-alkylthiophenes)

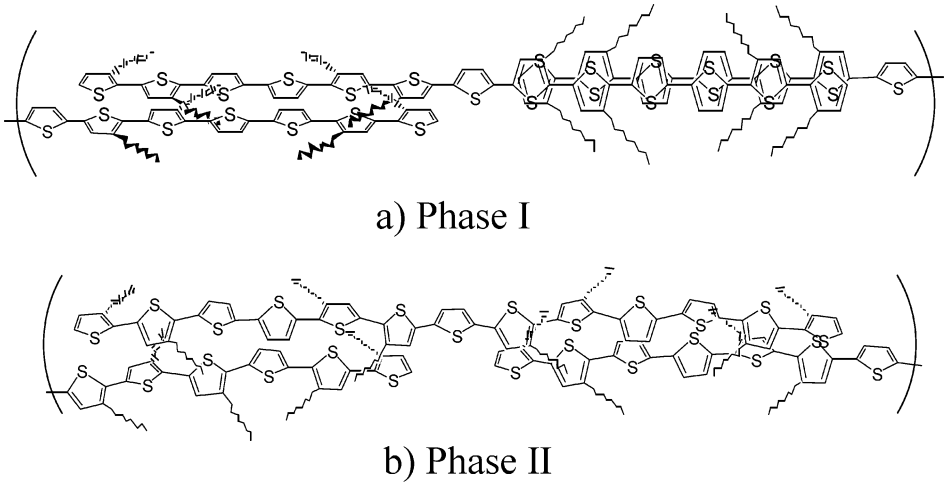

Figure 12. Conformational models proposed for 13T oligomers in (a) phase I and (b) phase II.

and poly(3-alkoxythiophenes) exhibit unresolved shoulders and side peaks on the long wavelength side of the main $\pi-\pi^*$ absorption band.[38−43] These fine structures are assigned to either a distribution of different π-conjugation lengths or vibronic structures, and have never been observed with unsubstituted polythiophenes. Fichou et al. have worked on absorption spectra of polycrystalline thin films of α-oligothiophenes.[32] They have found that the fundamental $\pi-\pi^*$ band for either of these oligomer films exhibits a succession of equally spaced side peaks on the low energy side. The energy spacing is 0.194 eV, compared well with 0.19 eV for the pristine 13T films. On the basis of careful discussions, these side peaks are ascribed to a coupling of the $\pi-\pi^*$ transition with vibrational levels of the excited state. Furthermore, these authors have concluded that the vibronic contributions arise from the quasiplanar and rigid-rod conformation of these α-oligothiophenes in the solid state, and this conformation is controlled by intermolecular interactions. On these bases, together with electrochemical data, one can presume that the half unit of the 13T oligomer in phase I, which prevails in pristine and relatively thick films, has a quasiplanar and rigid-rod conformation similar to that of the α-oligothiophenes in the solid state. On the other hand, after the bipolaron formation or the shift from phase I to phase II, the vibronic structures disappear entirely. No vibronic structures in the optical spectra of 13T films in phase II suggest that 13T oligomers whose π-conjugation length is increased to the full length of 13T have a nonplanar conformation. CV curves of Figure 4 for thin and pristine 13T films denote that a 13T film as thin as 3 nm consists almost of phase II and its fraction decreases as the 13T film thickness increases. Just like absorption spectra of 13T films after bipolaron formation, the absorption spectrum of the extremely thin 13T film shows a single broad band centered at 500 nm (Figure 7), similar to that of 13T in solution. It is quite likely that more stretched chains and thus longer conjugation units will be favored by an attractive interaction between sulfur atoms in oligothienylenes and a substrate such as gold. As the film thickness increases, the main absorption band tends to split into several peaks, suggesting an increased fraction of phase I. Such a spectral change with the film thickness is consistent with a view that phase I has a quasiplanar conformation assisted by a $\pi-\pi$ interaction between adjacent oligothiophenes, whereas phase II has a nonplanar conformation.

By summarizing the above arguments, we propose a conformational model schematically shown in Figure 12 for 13T oligomers in the solid state. In a pristine and relatively thick 13T film, the oligomer in the neutral state is twisted along the main chain at its center, and two halves of the nearby 13T oligomers are stacked by ring−ring interactions to give a somewhat planar conformation (Figure 12a). In this quasiplanar conformation, the 13T film has a redox nature similar to the one for the 6T film and may give rise to side peaks in the absorption spectrum due to intrachain vibronic contributions. By cycling the potential of the pristine 13T film between −0.1 and 0.5 V, π-dimers are reversibly formed between the adjacent two half segments, giving a stable redox wave at 0.40/0.25 V. When the 13T film is oxidized at potentials beyond 0.7 V, bipolarons are generated on the 6T units of the 13T oligomers. Immediately after the formation of bipolarons having planar quinoid structures on the 6T segments, the quinoid structure extends over the full unit of the 13T oligomer, and consequently, the twisted conformation breaking π-conjugation at the center of 13T is dissolved. The resulting 13T oligomers have full conjugation lengths. This conformational change is irreversible, so that the second oxidation peak at ca. 0.7 V observed with the pristine film disappears in the subsequent cycles. When the film that has once experienced the bipolaron formation is reduced to the neutral state, the 13T oligomers interact to a lesser extent with each other and show optical features of nonplanar oligomers (Figure 12b). The change in conformation of 13T leads to a change in morphology of the neutral 13T film, as clearly noted in the AFM images of Figure 10. The somewhat stretched neutral 13T oligomers undergo a redox reaction at less positive potentials than the pristine film because of the extension of the π-conjugation length. When they are oxidized again, one can expect the generation of two polarons on the respective chains of 13T oligomers, as discussed by Brédas et al.[44] The film obtained after the bipolaron generation is at a quasistable state, and 13T oligomers change their conformation to an original twisted one with a lapse of time or by $\pi-\pi^*$ excitation of the oligomer. Furthermore, the change from a planar (stacking) to a nonplanar (random) conformation induced by heating is consistent with a positive value of entropy for this conformational change.

Similar electrochemical and optical investigations were also made with oligoalkylthiophenes having 20 and 27 thienylene units (20T and 27T). Main oxidation peaks appeared at 0.45 and 0.40 V for 20T and 27T, respectively, but neither redox potential shift nor spectral change were observed. This finding implies that an unusual electrochemical response is proper to the 13T films whose oxidation potentials yielding polarons and bipolarons are placed adequately.

Conclusions

In spun films of 13T, the oligomer is twisted at its central position and has an effective π-conjugation length corresponding to sexithiophene. Adjacent half units of the twisted 13T oligomers are interacted so as to give a quasiplanar conformation, thus yielding vibronic side peaks together with a fundamental absorption band. Electrochemical generation of bipolarons on the 6T units in a pristine 13T film leads to a change in conformation of 13T through the formation of a quinoid structure, resulting in cancellation of the twisted conformation, and thus, the enhancement of the effective π-conjugation length. Because of this conformational change, the oxidation process in the resulting 13T film becomes more facile than in the pristine film and optical features of the oligomer film change accordingly.

References and Notes

(1) Roncali, J. *Acc. Chem. Res.* **2000**, *33*, 147.
(2) Quillard, S.; Corraze, B.; Poncet, M.; Mevellec, J. Y.; Buisson, J. P.; Evain, M.; Wang, W.; MacDiarmid, A. G. *Synth. Met.* **2003**, *137*, 921.
(3) Dimitrakopoulos, C. D.; Malenfant, P. R. L. *Adv. Mater.* **2002**, *14*, 99.
(4) Horowitz, G. *J. Mater. Chem.* **1999**, *9*, 2021.
(5) Bao, Z. *Adv. Mater.* **2000**, *12*, 227.
(6) Horowitz, G.; Hajlaoui, M. E. *Adv. Mater.* **2000**, *12*, 1046.
(7) Videlot, C.; Kassmi, A. El.; Fichou, D. *Sol. Energy Mater. Sol. Cells* **2000**, *63*, 69.
(8) Shaheen, S. E.; Brabec, C. J.; Sariciftci, N. S.; Padinger, F.; Fromherz, T.; Hummelen, J. C. *Appl. Phy. Lett.* **2001**, *78*, 841.
(9) Hoeve, W. ten; Wynberg, H.; Havinga, E. E.; Meijer, E. W. *J. Am. Chem. Soc.* **1991**, *113*, 5887.
(10) Sato, M.; Hiroi, M. *Polymer* **1996**, *37*, 1685.
(11) Yassar, A.; Delabouglise, D.; Hmyene, M.; Nessak, B.; Horowitz, G.; Garnier, F. *Adv. Mater.* **1992**, *4*, 490.
(12) Bäuerle, P.; Fischer, T.; Bidlingmeier, B.; Stabel, A.; Rabe, J. P. *Angew. Chem., Int. Ed. Engl.* **1995**, *34*, 303.
(13) Malenfant, P. R. L.; Groenendaal, L.; Fréchet, J. M. *J. Am. Chem. Soc.* **1998**, *120*, 10990.
(14) Mustafa, A. H.; Shepherd, M. K. *Chem. Commun.* **1998**, 2743.
(15) Nakanishi, H.; Sumi, N.; Aso, Y.; Otsubo, T. *J. Org. Chem.* **1998**, *63*, 8632.
(16) Sumi, N.; Nakanishi, H.; Ueno, S.; Takimiya, K.; Aso, Y.; Otsubo, T. *Bull. Chem. Soc. Jpn.* **2001**, *74*, 979.
(17) Otsubo, T.; Aso, Y.; Takimiya, K. *Bull. Chem. Soc. Jpn.* **2001**, *74*, 1789.
(18) Izumi, T.; Kobashi, S.; Takimiya, K.; Aso, Y.; Otsubo, T. *J. Am. Chem. Soc.* **2003**, *125*, 5286.
(19) Ohshita, J.; Watanabe, T.; Kanaya, D.; Ohsaki, H.; Ishikawa, M.; Ago, H.; Tanaka, K.; Yamabe, T. *Organometallics* **1994**, *13*, 5002.
(20) Tanaka, K.; Ago, H.; Yamabe, T.; Ishikawa, M.; Ueda, T. *Organometallics* **1994**, *13*, 5583.
(21) Kunai, A.; Ueda, T.; Horata, K.; Toyoda, E.; Ohshita, J.; Ishikawa, M.; Tanaka, K. *Organometallics* **1996**, *15*, 2000.
(22) Harima, Y.; Kunugi, Y.; Tang, H.; Yamashita, K.; Shiotani, M.; Ohshita, J.; Kunai, A. *Synth. Met.* **2000**, *113*, 173.
(23) Jiang, X.; Harima, Y.; Zhu, L.; Yamashita, K.; Naka, A.; Lee, K. K.; Ishikawa, M. *J. Mater. Chem.* **2003**, *13*, 785.
(24) Harima, Y.; Jiang, X.; Kunugi, Y.; Yamashita, K.; Naka, A.; Lee, K. K.; Ishikawa, M. *J. Mater. Chem.* **2003**, *13*, 1298.
(25) Barth, M.; Guilerez, S.; Bidan, G.; Bras, G.; Lapkowski, M. *Electrochim. Acta* **2000**, *45*, 4409.
(26) Lapkowski, M.; Sadlok, M. K.; Zak, J.; Guillerez, S.; Bidan, G. *Adv. Mater.* **2001**, *13*, 803.
(27) Domagala, W.; Lapkowski, M.; Guillerez, S.; Bidan, G. *Electrochim. Acta* **2003**, *48*, 2379.
(28) Lapkowski, M.; Zak, J.; Sadlok, M. K.; Guillerez, S.; Bidan, G. *Electrochim. Acta* **2001**, *46*, 4001.
(29) Meerholz, K.; Heinze, J. *Angew. Chem., Int. Ed. Engl.* **1990**, *29*, 692.
(30) Zotti, G.; Schiavon, G.; Berin, A.; Pagani, G. *Adv. Mater.* **1993**, *5*, 551.
(31) Feldberg, S. W. *J. Am. Chem. Soc.* **1984**, *106*, 4671.
(32) Fichou, D.; Nunzi, J. M.; Charra, F.; Pfeffer, N. *Adv. Mater.* **1994**, *6*, 64.
(33) In preparation.
(34) Guay, J.; Kasai, P.; Diaz, A.; Wu, R.; Tour, J. M.; Dao, L. H. *Chem. Mater.* **1992**, *4*, 1097.
(35) Bäuerle, P.; Segelbacher, U.; Maier, A.; Mehring, M. *J. Am. Chem. Soc.* **1993**, *115*, 10217.
(36) Yu, Y.; Gunic, E.; Zinger, B.; Miller, L. *J. Am. Chem. Soc.* **1996**, *118*, 1013.
(37) Guay, J.; Kasai, P.; Diaz, A.; Wu, R.; Tour, J. M.; Dao, L. H. *Chem. Mater.* **1992**, *4*, 1097.
(38) Rughooputh, S. D. D. V.; Hotta, S.; Heeger, A. J.; Wudl, F. *J. Polym. Sci.* **1987**, *25*, 1071.
(39) Salaneck, W. R.; Inganäs, O.; Thémans, B.; Nilsson, J. O.; Sjögren, B.; Österholm, J. E.; Brédas, J. L.; Svensson, S. *J. Chem. Phys.* **1988**, *89*, 4613.
(40) Yoshino, K.; Nakajima, S.; Gu, H. B.; Sugimoto, R. *Jpn. J. Appl. Phys.* **1987**, *26*, L1371.
(41) Schweizer, K. S. *J. Chem. Phys.* **1986**, *85*, 1156.
(42) Daoust, G.; Leclerc, M. *Macromolecules* **1991**, *24*, 455.
(43) Roncali, J. Youssoufi, H. K.; Garnier, R.; Lemaire, M. *J. Chem. Soc., Chem. Commun.* **1990**, 414.
(44) van Haare, J. A. E. H.; Havinga, E. E.; van Dongen, J. L. J.; Janssen, R. A. J.; Cornil, J.; Brédas, J. *Chem.—Eur. J.* **1998**, *4*, 1509.